Lawrence Berkeley National Laboratory
LBL Publications

Title
New horizons in thermoelectric materials: Correlated electrons, organic transport, machine learning, and more

Permalink

Journal

ISSN

Authors
Urban, Jeffrey J
Menon, Akanksha K
Tian, Zhiting
et al.

Publication Date

DOI

Jeffrey J. Urban, Akanksha K. Menon, Zhiting Tian, Anubhav Jain, and Kedar Hippalgaonkar

COLLECTIONS

Note: This paper is part of the special topic on Advanced Thermoelectrics.

F This paper was selected as Featured

View Online   Export Citation   CrossMark

ARTICLES YOU MAY BE INTERESTED IN

Tomorrow's micromagnetic simulations
Journal of Applied Physics **125**, 180901 (2019); https://doi.org/10.1063/1.5093730

Phonon properties and thermal conductivity from first principles, lattice dynamics, and the Boltzmann transport equation
Journal of Applied Physics **125**, 011101 (2019); https://doi.org/10.1063/1.5064602

Experimental evidence for the separation of thermally excited bipolar charge carries within a p-n junction: A new approach to thermoelectric materials and generators
Journal of Applied Physics **125**, 184502 (2019); https://doi.org/10.1063/1.5081998

New horizons in thermoelectric materials: Correlated electrons, organic transport, machine learning, and more Ⓕ

Jeffrey J. Urban,[1,a) 🆔 Akanksha K. Menon,[2] Zhiting Tian,[3] Anubhav Jain,[2] and Kedar Hippalgaonkar[4] 🆔

AFFILIATIONS

[1]The Molecular Foundry, Lawrence Berkeley National Laboratory, Berkeley, California 94720, USA
[2]Energy Storage and Distributed Resources Division, Lawrence Berkeley National Laboratory, Berkeley, California 94720, USA
[3]Sibley School of Mechanical and Aerospace Engineering, Cornell University, Ithaca, New York 14853, USA
[4]Institute of Materials Research and Engineering, Agency for Science Technology and Research, #08-03, 2 Fusionopolis Way, Singapore 138634

Note: This paper is part of the special topic on Advanced Thermoelectrics.
[a)]**Author to whom correspondence should be addressed:** jjurban@lbl.gov

ABSTRACT

Thermoelectrics represent a unique opportunity in energy to directly convert thermal energy or secondary waste heat into a primary resource. The development of thermoelectric materials has improved over the decades in leaps, rather than by increments—each leap forward has recapitulated the science of its time: from the crystal growth of semiconductors, to controlled doping, to nanostructuring, and to 2D confinement. Each of those leaps forward was, arguably, more a result of materials science than physics. Thermoelectrics is now ripe for another leap forward, and many probable advances rely on new physics outside of the standard band transport model of thermoelectrics. This perspective will cover a limited selection of how thermoelectrics can benefit from new discoveries in physics: wave effects in phonon transport, correlated electron physics, and unconventional transport in organic materials. We also highlight recent developments in thermoelectrics discovery aided by machine learning that may be needed to realize some of these new concepts practically. Looking ahead, developing new thermoelectric physics will also have a concomitant domino effect on adjacent fields, furthering the understanding of nonequilibrium thermal and electronic transport in novel materials.

I. INTRODUCTION

Thermal energy is a valuable often overlooked resource in the energy economy—rather than a mere dissipative consequence of an irreversible work cycle, it can itself serve as a source of energy. While massive funding efforts have been deployed to accelerate the development of different forms of energy such as solar energy (photovoltaics), electrical energy storage (batteries), and chemical energy (electrocatalysis, CO_2 conversion), thermal energy is easily overshadowed. However, thermal energy is a titan in the shadows, as over 60% of primary energy usage in the United States in 2017 resulted in thermal energy production, a staggering 67 Quadrillion BTU worth, equivalent to 2200 Gigawatt-years of energy.[1] Axiomatically, thermal energy is underlying every system that performs work or is otherwise plagued by low efficiency—the most common pathways of dissipation involve heat of some type, and efforts to make systems "more efficient" often boil down to ways to engineer or to control thermal energy dissipation.

Thermoelectrics are solid-state materials that directly convert thermal energy into electrical energy and provide a potentially vital resource in a future energy economy where increasingly every Joule is precious. Thermoelectrics have traditionally been viewed as a way to squeeze out a bit of extra energy by partnering them as a secondary energy conversion modality in very high-temperature low-efficiency processes such as production of steel, glass, etc. Thus, thermoelectrics have largely been relegated to niche applications where other energy sources are not readily available (submarines, deep space, etc.). This has been an entrenched view, often viewed as unavoidable due to Carnot considerations, that one needs high hot-side temperatures

to allow for traditionally inefficient thermoelectrics to provide enough useful payback to justify investing in their synthesis and installation. This view is incomplete at best and founded upon a notion of thermoelectrics that has its origin in centuries old transport formalisms built to capture the physics of doped semiconductors. However, there are several emerging areas in physics that are not well-described by these models—new insights into topological states, correlated electron physics, and transport in organic semiconductors, to name a few. Furthermore, new tools such as machine learning and computational screening can accelerate the rate at which these new principles may be translated into practical materials systems.

Moreover, as of 2016, approximately 85% of work potential from all waste heat sources in the United States come from sources at or below 400 °C, so there is increasing impetus to uncover ways to harness this resource.[2] Thermodynamically, this is judicious, as we primarily combust fossil fuels at high temperature (>1000 °C) to provide thermal energy for low-temperature needs such as residential heating;[2] this invokes a massive and unnecessary exergetic penalty. Thus, both the recent advances in physics and new dynamics of the energy economy in the 21st century argue for a refreshed perspective on what thermoelectrics are needed for in the future—what kinds of materials properties (bandgap, effective mass, thermal conductivity, etc.) would be ideal for capturing and converting energy from increasingly diffuse, low-temperature sources? Epistatic upon these new insights is the observation that thermoelectrics may also play a pivotal role in new sectors that were never imagined a century ago—implantable medical devices, remote sensor networks, the Internet-of-Things—these new demands also create a thirst for new types of thermoelectrics to meet these emergent applications.

This perspective will reprise the essential advances in physics relevant to thermoelectrics and point toward what kinds of new materials are poised to meet these challenges and what seminal questions still remain to be addressed. We begin by revisiting the historical conception and essential physics of thermoelectrics—how the Boltzmann transport equation and assumptions of isotropic, free-electron gases can explain much of the phenomenology of thermoelectrics to date, and what limitations those notions place on further advancement. We then showcase promising horizons in physics and point to how these new concepts can be transformative. A decade from now, for instance, one might envision making thin, lightweight, flexible thermoelectric device architectures comprised of earth abundant materials—one might even call these "anti-thermoelectrics" as they challenge the conventional notion of what a thermoelectric module looks like.[3–8] Nothing in physics prevents this, yet most thermoelectrics are thick, brittle, rigid, and depend upon relatively scarce elements such as bismuth, tellurium, and selenium. We also describe what physics allows decoupling of the historically entangled thermoelectric parameters of electrical conductivity, Seebeck coefficient, and thermal conductivity. To achieve this, we will weave together important subdisciplines of solid-state physics, computation and modeling, and materials science.

II. HIDDEN ASSUMPTIONS IN "THE STANDARD MODEL" OF THERMOELECTRICS

A brief recent history of thermoelectrics recapitulates progress in many areas of science, as exemplified by Thomas Kuhn's work on scientific revolutions—there have been long stretches (i.e.,

decades) of time where performance across a wide range of materials (as benchmarked by figure of merit, ZT) has essentially been stagnant, then new paradigms (such as nanostructuring) appear, and rapid progress is made across many classes of materials, and then another plateau is hit. ZT is defined as

$$ ZT = \frac{S^2 \sigma}{(\kappa_{ph} + \kappa_e)} T, \tag{1} $$

where S is the Seebeck coefficient, σ is the electrical conductivity, κ_{ph} is the thermal conductivity due to phonons (lattice vibrations), and κ_e is the heat carried by the charges (this includes contributions from both electrons and holes and is predominantly dominated by electrons in n-type materials and by holes in p-type materials) at a thermodynamic temperature, T. Figure 1 shows the progress in thermoelectric material development over time across three classes of materials, namely, inorganic semiconductors, conducting polymers, and organic–inorganic hybrids, which highlight the variety and diversity of materials systems that have been identified as thermoelectrics. It is worth mentioning that while inorganic materials such as bismuth telluride (Bi_2Te_3) have been studied since 1940s, polymer-based materials have been reported only in the last decade; their inherently low thermal conductivity, unique transport characteristics, and tunable electronic properties are promising and will be discussed in a later section.

Currently, there is an energetic search going on for new physical paradigms to propel thermoelectric materials forward again. From the 1950s until the late 1990s, thermoelectric development was in stasis with a few gains in overall ZT. During this time, there was a belief that the transport equations governing standard doped semiconductor thermoelectrics (i.e., the Boltzmann transport equations, henceforth abbreviated BTE) limited overall ZT due to the fundamental interdependence of the transport phenomena. However, in the late 1990s and early 2000s, many new concepts emerged to challenge this notion. One idea that had an enormous impact was predicated on the essential realization that a significant fraction of phonon mean free paths (mfp) tend to be an order of magnitude or so larger than electron mean free paths.[29–31] Thus, by creating materials with grain sizes intermediate between these two transport regimes (i.e., larger than electron mfp but smaller than the majority of phonon mfp), one could confer some reduction in thermal conductivity without detracting too much from the electronic conductivity or Seebeck, delivering a net boost to ZT. Often, this optimum length scale ended up being on the order of tens to hundreds of nanometers, and this design concept became known as nanostructuring. This concept, in general, worked well and propelled many materials past a mythical barrier of $ZT \sim 1$ (at least at the lab scale) and showed that it was indeed possible to disentangle—to some degree—the thermal and electrical portions of ZT. Since that time, many different avenues have been pursued to realize further boosts to ZT—spin entropy, quantum correlations, low-dimensional transport, etc. While there have been selective reports of individual materials realizing new record levels of performance (as high as $ZT \sim 2.6$) in lab scale $SnSe$[32] and Cu_2Se,[33] no general approach has emerged from these studies and it is unclear whether these materials can be deployed broadly, so the field remains ripe for innovation. Here, we
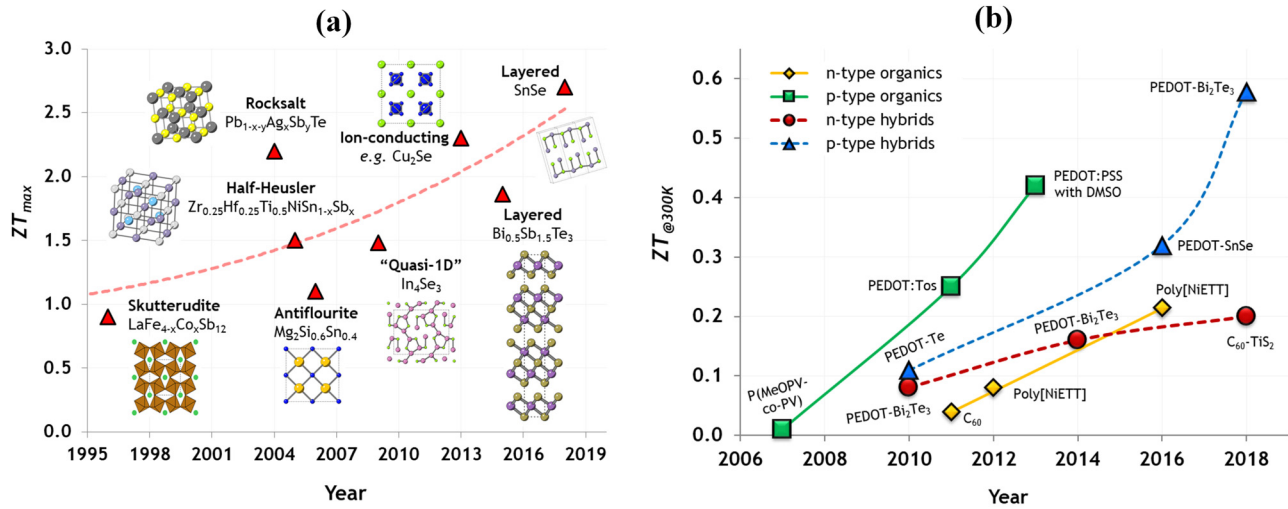
FIG. 1. (a) Progress of maximum figure of merit (*ZT*) in bulk inorganic systems achieved over time, highlighting the diversity of chemical systems and mechanisms that have shown high performance.[9–16] (b) Progress of *ZT* at room temperature (300 K) in p- and n-type organic materials[17–22] and organic–inorganic hybrid systems[23–28] over time, highlighting the rapid advancements in materials based on poly(3,4-ethylenedioxythiophene) or PEDOT. Here, P(MeOPV-*co*-PV) is poly (2,5-dimethoxyphenylenevinylene-*co*-phenylenevinylene), Tos is tosylate, PSS is poly(styrenesulfonate), C_{60} is fullerene, and poly(NiETT) is poly(nickel-ethenetetrathiolate).

outline a few opportunities to increase *ZT* based upon emerging concepts in physics that could have a substantial impact.

III. VIOLATING THE WIEDEMANN–FRANZ LAW

Conventional thermoelectric materials are inorganic semiconductors, and charge conduction is well-described by band transport derived from the Boltzmann transport theory.[34] The essential transport parameters underlying thermoelectric performance are depicted in Fig. 2. In these systems, the electrical conductivity is expressed as

$$\sigma = e^2 \int \tau v^2 g \left(-\frac{\partial f_0}{\partial E} \right) dE, \qquad (2)$$

where *e* is the elemental charge, *v* is the carrier velocity, τ is the scattering time, *g* is the electronic density of states (henceforth abbreviated as DOS), f_0 is the equilibrium Fermi-Dirac distribution, and *E* is the energy of the charge carriers. These terms are also present in the expression for the Seebeck coefficient,

$$S = \frac{k_B}{e} \frac{\int \tau v^2 g \left(\frac{E - E_F}{k_B T} \right) \left(-\frac{\partial f_0}{\partial E} \right) dE}{\int \tau v^2 g \left(-\frac{\partial f_0}{\partial E} \right) dE}, \qquad (3)$$

where k_B is the Boltzmann constant and E_F is the Fermi level or chemical potential that can be tuned via doping. This expression provides a physical interpretation of the Seebeck coefficient, i.e., it is a measure of the asymmetry in the distribution of electrons with energy greater than E_F (hot electrons) and those with lower energy

(cold electrons), thereby a direct representation of the entropy per charge carrier. The expression also shows the inverse relationship between *S* and σ, and this coupling makes it challenging to obtain high power factors ($S^2\sigma$) in most thermoelectric materials. *S* can be enhanced (for n-type thermoelectrics) by moving the Fermi level far from the conduction band to increase asymmetry; however, this results in a decrease in σ as fewer carriers are available for transport. Strategies to decouple *S* and σ have been investigated in inorganic semiconductors, and these typically exploit either perturbations to the electronic density of states or different scattering mechanisms (e.g., resonant states in bulk materials, sharp DOS in low-dimensional materials,[35,36] or modulation doping).[37]

The fundamental assumptions of the BTE model artificially constrain parameter optimization in thermoelectrics, however, as there is no obvious reason that all thermoelectrics should be so well-described by a formalism that relies on systems being described by one predominant characteristic relaxation time dominated by 3D free-electron motion and electron–phonon scattering. Within the BTE, an energy-independent, constant scattering time assumption is commonly employed to predict the behavior of high-performance thermoelectric materials. However, this assumption is usually far from the truth,[38] even for conventionally doped semiconductors that follow Fermi liquid behavior. For instance, in bulk solids, electron–phonon scattering is often considered the dominant mechanism underlying transport, which equates to a relaxation time approximated as $\tau \propto E^r$, where $r = -1/2$ (typical for acoustic deformation potential scattering in 3D). At high levels of doping, where an optimized value of power factor typically occurs, the scattering can be dominated by ionized impurities, which can result in a strong energy dependence of charge scattering ($r = 3/2$).[39] This is vital as the nature of the dominant scattering processes for electrons
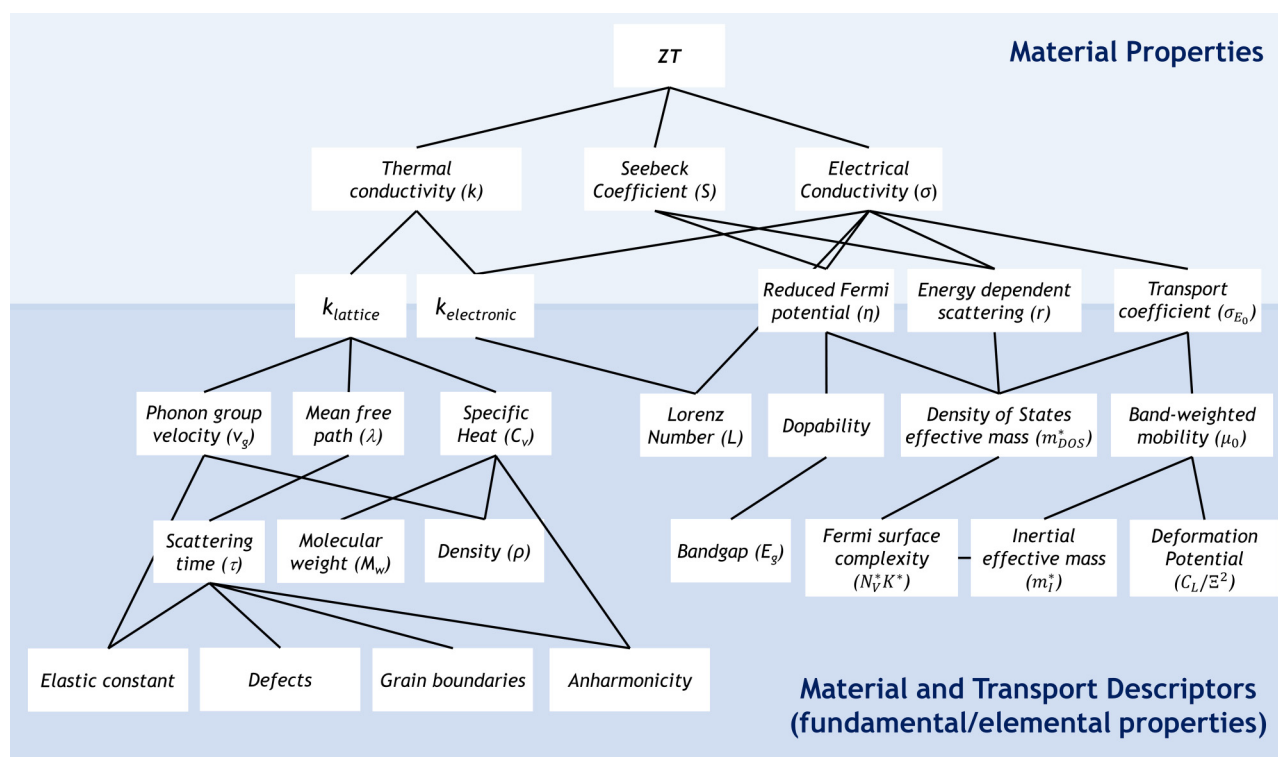
FIG. 2. A thermoelectrics knowledge map describing key material properties as well as intrinsic transport and materials descriptors that are interdependent—some can be experimentally measured and others can be calculated theoretically. A rational data-driven approach that provides a framework for predicting and producing new thermoelectric materials has to address not only material design, but also microstructure and scattering (nonequilibrium) design.

underlies a crucial parameter in the physics of thermoelectrics optimization called the Lorenz number. This Lorenz number, L, relates the electronic thermal conductivity to the electrical conductivity ($L = \kappa_e/\sigma T$); this is referred to as the Wiedemann–Franz Law. The single-particle Wiedemann–Franz law predicts a Sommerfeld value of $\frac{\pi^2}{3}\left(\frac{k_B}{e}\right)^2$ for L, assuming no energy dependence of scattering.[34] The figure of merit can be rewritten as $ZT = \frac{S^2/L}{(1+\kappa_{ph}/\kappa_e)}$. Therefore, a deviation away from the Wiedemann–Franz law where L is lower than the Sommerfeld value is favorable for thermoelectrics as this corresponds to a case where electrons can carry charge, but little heat. For Fermi liquids, a lower energy dependence of scattering times ($r < -1/2$) is the precondition that enables such exploration.[39] Another opportunity to reduce the Lorenz number is by looking for or designing new materials that have sharp density of states near the band extrema, and multiple bands at the same energy, promoting intervalley scattering.[40,41] Figure 2 depicts a map of different transport descriptors and their interdependence, which manifests as correlated material properties.

Nonfermi liquids, correlated electron materials, and scattering events between charged and neutral species (gapless excitations, e.g., magnons, etc.) could affect charge and heat currents differently. Many examples of this exist and provide a direct lever for

manipulating the reformulated ZT via the Lorenz number. However, most of these deviations manifest as an increase of L, which is unfavorable for thermoelectrics. One such example is that of spin-charge separation in 1D Tomonaga–Luttinger liquids, which results in heat (carrier entropy) being carried efficiently by both spinons and holons, while electric current is only due to charge.[42] Another example occurs in Dirac fluids, or in charge-neutral electron-hole plasmas in 2D graphene; in these materials, the plasmas carry heat efficiently, but do not transfer charge current, thus resulting in a large L.[43] Closer to home for thermoelectrics is the coupling of heat and charge transport in conducting polymers, where the Lorenz number has been shown to be larger than the Sommerfeld value.[44,45] Avenues to transport in low Lorenz number regimes are rare, but do exist. A recent prominent example was metallic vanadium dioxide (VO_2), which showed that these desirable, ultralow values of L can be achieved[46] in strongly correlated "bad metals" where heat and charge both move by diffusion below the Mott–Ioffe–Regel limit (these are systems characterized by electron mfp defined by the Drude picture that are smaller than the lattice constant). Here, in the case of the correlated metallic state of VO_2, L is an order of magnitude smaller than the Sommerfeld value and the Seebeck coefficient is observed to be enhanced. This is
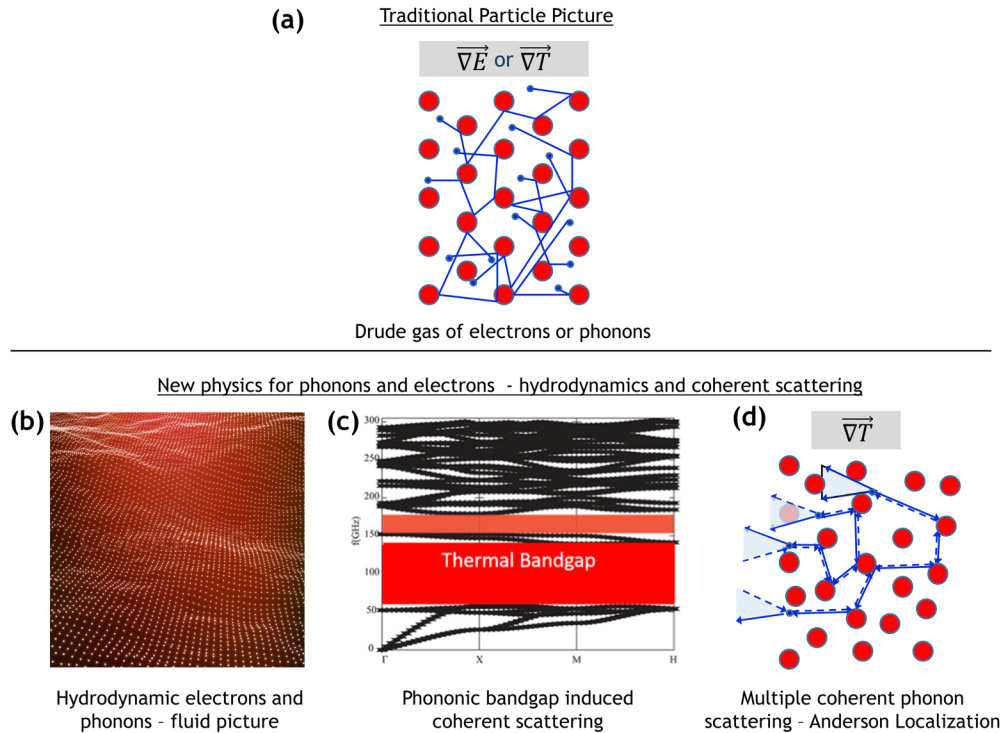
FIG. 3. Illustrations comparing the kinetic particle picture and the hydrodynamic (or coherent) picture of phonons and electrons. In (a), electrons and phonons behave like particles, and their transport out of equilibrium under a temperature or electric potential gradient can be described well by the kinetic gas Drude picture: here, the particles travel at a velocity with a mean free path that describes the average distance between collisions. In the hydrodynamic picture (b), they travel like a fluid, wherein interaction with fellow carriers is strong, and heat and/or electric current is carried via collective motion rather than as individual particles. (c) Illustration of the phonon dispersion relation in the case where a phononic (thermal) bandgap is formed when the phonon lattice has a periodic constant on the order of the phonon wavelength, therefore restricting heat flow. Adapted with permission from Zanjani and Lukes, J. Phys. Chem. C **119**(29), 16889–16896 (2015).[61] Copyright 2015 American Chemical Society. (d) Anderson localization of heat—a disordered solid where phonons undergo multiple scattering events, where each event is coherent (phase-preserving), resulting in maximum backscattering.

because the electrons move as a collective hydrodynamic fluid [Fig. 3(b)] where the thermal and electrical diffusivities are identical and charge moves effectively, while heat is dissipated. In the incoherent metal picture (collective transport), conductivity is not determined by particle relaxation rates, but instead by diffusion coefficients:[47] such physics allows for effective charge and heat separation, providing a new knob to tune the Lorenz number. This is akin to the Lewis number in fluids, which is defined as the ratio of thermal diffusivity to the mass diffusivity. Empirically, it has been observed that a low Lewis number in mixed-gas combustion can result in flame balls, where heat does not flow efficiently, but the fluid front moves collectively like a ball.[48] Exploration of novel correlated systems that exhibit rich physics will certainly push the field of thermoelectrics to new frontiers of discovery.

IV. WAVE EFFECTS IN PHONON TRANSPORT

Historically, electron and phonon transport for thermoelectrics has predominantly been viewed using the particle picture. One emerging area in the physics of thermoelectrics is taking advantage of their wave effects to reach higher ZT values. Phonon transport in

nanostructures can be affected by diffuse interface scattering [Fig. 3(a)] or a coherent wave interference. While traditional nanostructuring is based on classical size effects ascribed to diffuse boundary scattering, the phonon wave picture has been much less investigated.[49–52] The main consequence of phonon interference is to modify the phonon dispersions, creating forbidden energy bandgaps for thermal phonons in analogy to photonic bandgap materials [Fig. 3(c)] and, in a disordered structure, to enable the possibility of multiple coherent scattering (such as Anderson localization of phonons) as illustrated in Fig. 3(d). Coherent phonon interference can, therefore, potentially establish a new basis to push the thermal conductivity below the lower limit prescribed in the phonon particle picture (without compromising electron transport) and enhance ZT values. While alluring, it remains incredibly challenging to take advantage of the thermal phonon bandgap to effectively reduce the major heat carrying modes. This is due to the intrinsic wavelengths of the thermal phonons involved, defined as $\lambda_{th} = h v_g / k_B T$, where v_g is the group velocity of acoustic phonons ($\sim 10^3$–10^4 m/s) that are predominantly responsible for carrying the heat; at room temperature in most materials, $\lambda_{th} \sim 1$–5 nm. To realize these wavelike effects, the macroscale dimensions need to be larger than the

localization length; however, the microscale structural periodicity needs to be smaller or comparable to the coherence length of phonons. This leads to ideal geometries which are patterned on the ~nm length scale over hundreds of micrometers—this is an extreme challenge for modern fabrication techniques. An important observation is that these length scales are a function of temperature and occupancy of phonons, and this provides an additional knob for a proof-of-concept demonstration of this phenomenon. It is not currently possible to reproducibly design structures to take advantage of these phononic effects, although there have been some lab scale reports that are promising[53,54] and the technology continues to evolve. For example, in terms of top-down fabrication, the bit-patterned media, atomic layer deposition (ALD), and He-ion[55] based approaches are enabling the ability to conceive of good phononic structures. However, these remain limited in scope and materials and cannot yet reach the shortest possible phonon wavelengths desired. In a complementary sense, recent advances in colloidal self-assembly of hybrid nanocrystals[56] hold great promise for phonon wave features to effectively reach the new thermal conductivity minimum, and there have been some reports of wavelike aspects in these systems.[57] When disorder in a material is strong, and scattering from such disorder preserves phase, then the phonons behave like waves resulting in multiple coherent scattering, unlocking the possibility of new physics such as Anderson Localization[58,59] where destructive interference of phonon waves prevents diffusion and instead causes localization of heat, as illustrated in Fig. 3.[51,60]

V. TRANSPORT IN ORGANIC AND HYBRID MATERIALS

Conducting polymers and hybrid organic-inorganic systems offer another promising avenue for future thermoelectrics development as they exhibit different electronic and thermal transport properties than traditional doped semiconductors; they possess nontraditional structure–property correlations that vary from the familiar doped, crystalline semiconductors that are the workhorses of thermoelectrics. One distinguishing feature of these systems is the extent of doping, which is much larger than in inorganic semiconductors—dopant concentrations can be up to 35% for

polymers compared to 1% for inorganics.[62] The other differentiating factor is the effect of doping—in addition to introducing carriers, doping also alters the transport landscape and creates energetic and spatial disorder that leads to carrier localization, which can be detrimental to transport. The presence of these localized states (i.e., polarons) challenges the application of the free-electron approximation that describes electronic transport in inorganic semiconductors, and a comprehensive understanding of transport in these disordered systems remains elusive. For example, while Hall measurements could yield information on the carrier effective mass, which gives insight into the band structure and underlying transport properties, correct implementation and interpretation of the Hall coefficient remains a challenge (Hall effect relies on delocalized carriers with well-defined cyclotron orbits smaller than the mean free path/grain size).[63,64] More applicable to these materials are transport models for disordered systems with localized carriers such as Mott's mobility-edge and variable range hopping formalism developed for amorphous silicon and inorganic alloys.[65,66] Unfortunately, these models do not provide consistent fits to the Seebeck coefficient and electrical conductivity data for polymers: this is expected as such models were developed for homogeneous samples with a constant DOS, while doped polymers show large variations (e.g., molecular weight, crystallinity, role of counterion after doping, etc.), as well as microscale heterogeneity and changes in DOS with doping.[67] Despite these challenges, the coupling between phononic and electronic degrees of freedom in polymers and their morphology provides new opportunities toward breaking the S-σ anticorrelation that plagues doped inorganic semiconductors. For example, conducting polymers are found to deviate from, and violate, the Wiedemann–Franz law, and their electrical and thermal conductivity values are found to be highly morphology dependent while the Seebeck coefficient largely depends on the energy landscape, as shown in Fig. 4.[68,69]

Furthermore, there is a scaling of Seebeck coefficient and electrical conductivity in many of the best performing materials.[70,71] In the absence of a comprehensive model to explain these transport trends in polymeric thermoelectrics, the Kang–Snyder empirical model provides some insight by prescribing a transport function, σ_E
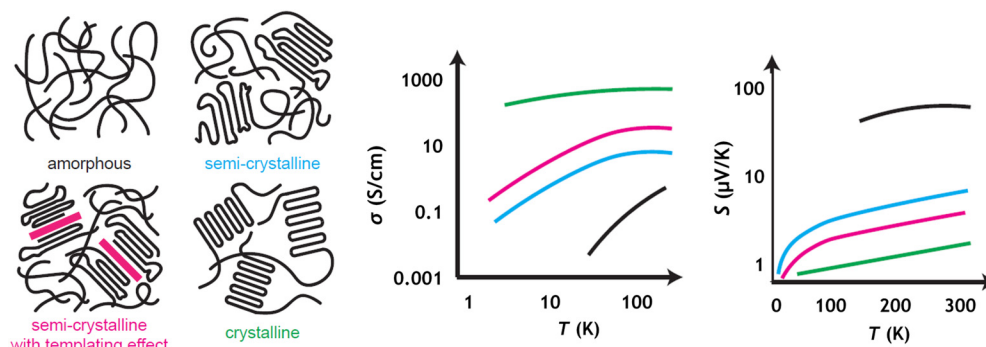

FIG. 4. Illustrations of different morphologies in organic materials that result in varying degrees of electron–phonon coupling. The extent of spatial and energetic disorder in organic materials and in organic–inorganic hybrid systems results in different temperature trends for electrical conductivity and Seebeck coefficient (color-coded to the four structures). The transport properties can be highly anisotropic in these materials and are sensitive to the processing conditions and measurement direction.

that captures the temperature and energy dependence of charge transport across a wide range of polymers through two fitting parameters, σ_{E_0} (analogous to an effective carrier mobility) and s (dependent upon DOS and scattering).[72] The best performing thermoelectrics are based on poly(3,4-ethylenedioxythiophene) (PEDOT) which shows $s = 1$, while most other doped polymers follow $s = 3$.[72] The extent of electron–phonon coupling and the dominant scattering mechanism could possibly be a contributor to different s values in polymers. Devising a system where the electron–phonon coupling can be tuned systematically to probe the resulting charge transport is highly desired—for instance, by tailoring dopants for a specific polymer (through introducing suitable side chains), or by extending the carrier concentration window through electrostatic or electrochemical gating in FETs and organic electrochemical transistors (OECTs), respectively,[73,74] to achieve the optimum doping level. In a complementary sense, recent advances in intrinsic conductors, such as self-doped perylene diimides (PDIs)[75] and metal-coordinated polymers such as nickel-ethenetetrathiolate or poly(NiETT),[22,76–80] show promise to glean insight into transport physics in polymers without encountering the challenges of doping (low doping efficiencies and the ill-defined role of the counterion in charge transport).

Another avenue for next generation thermoelectric materials is the development of hybrid materials. A distinguishing feature of hybrid materials (in contrast to composites or material mixtures) is that the overall ZT of the hybrid organic/inorganic system can surpass that of either individual component. While this seemingly contradicts intuition derived from simplistic effective media models such as Berman-Fel[81] or Bergman-Levy,[82] those theories do not account for physical interactions between components and, for example, fail to predict the effects of dopants in silicon. It should, therefore, not be surprising that highly interacting hybrid materials can exhibit ZTs that surpass the individual components comprising it. One embodiment of this is a polymer blend or copolymer with carefully designed energy levels and controlled/selective doping to offset the Fermi level from the transport level, thereby allowing for a simultaneous increase in Seebeck and electrical conductivity.[83,84] Another embodiment of a hybrid material is based on new phases of materials that conjoin inorganic and organic materials that have shown simultaneous improvement in S and σ.[85] Energy filtering at the interface has been incorrectly posited in many of these systems; energy filtering requires an energy barrier between intermixed metallic and semiconductor phases, allowing cold electrons to be selectively filtered out, while the hot electrons contribute to an enhanced Seebeck coefficient (while mildly reducing the electrical conductivity).[86] The challenge with achieving energy filtering stems from the fact that a "true hybrid," which shows strong chemical interactions between the organic and inorganic phases, is difficult to make. Most formulations in the literature leverage a change in polymer morphology to enhance electrical conductivity (i.e., a templating of the organic phase on the inorganic, Fig. 4), along with charge transfer at the inorganic–organic interface. This does not result in a change in the electronic structure or the energy dependence of scattering, which are prerequisites for invoking energy filtering to enhance the power factor.[87] Hence, new synthesis routes that generate true inorganic–organic hybrid materials where the new material is different from and better than the original constituents remains an open challenge.

VI. NEW HORIZONS IN UNCONVENTIONAL THERMOELECTRIC MATERIALS—FINDING THE TREASURE THAT IS NOT ON THE MAP

As emphasized throughout our discussion, a key challenge that remains in developing advanced thermoelectric materials is to balance the traditionally competing properties that lead to a high ZT. As early as 2003, researchers such as Blake and Metiu recognized that computations may play an important role, envisioning "a time where one runs multiple computer test tube reactions like these on large Beowulf clusters—as a means of screening for new TE materials" and that "in the future, theory may be a very competent dance partner for what has previously been a solo experimental effort in searching for ever better TE materials."[88] Today, with the advent of high-throughput computing, machine learning, and artificial intelligence (AI) tools, it is now becoming increasingly viable to use algorithms to uncover new thermoelectric materials as a supplement to human intuition.[89] While these techniques are currently applied to conventional thermoelectrics discovery, they may likely be more targeted at identifying unconventional thermoelectrics in the future, as evident from the recent attempt to screen materials with low Lorenz number.[41]

The vision of large, computationally guided searches for thermoelectric materials was first realized in 2006 by Madsen.[90] In a pioneering study, Madsen used high-throughput computation to identify a promising n-type candidate material, LiZnSb, that ultimately was revealed to be p-type when subjected to experiment.[91] Since then, there have been many subsequent computational searches for thermoelectric materials and, enticingly, some of these theoretical papers suggest that ZTs might one day far surpass those of today's materials, perhaps with a $ZT > 5$.[92] A few of these computational searches have led to experimental confirmations of previously unknown thermoelectric compositions, as summarized in Table I. Expanding the role and scope of theory-experiment collaborations would likely lead to many more such confirmed instances of thermoelectric predictions in the future.

Despite the many advances, it remains difficult to efficiently and accurately compute many TE properties. A host of techniques at various levels of computational complexity have been developed to compute or estimate both electronic and thermal transport properties[107–111] (for a review, see Ref. 112). As might be expected, the more accurate methods generally tend to be computationally expensive or difficult to automate, whereas the simpler techniques often only provide a qualitative ranking between thermoelectric compounds.[113] There is still room in the field to develop techniques that provide greater accuracy at lower computational cost. Especially interesting are the extension of such models to include boundary scattering and dimensionality effects, geometric shape factors, and anisotropy.

Typically, regardless of technique, the thermoelectric viability of a candidate is generally treated as an intrinsic materials property. This assumption is also reflected in "quality factor" (β-factor[114] or the B-factor)[115] and related approaches.[116,117] Traditionally, the quality factor has described a good material as $\beta \propto \mu_0 m^{*3/2}/k_L$, which encompasses the central materials challenge of designing a material with high mobility, μ_0 while still possessing a large density-of-states effective mass, m^* to enhance the Seebeck

TABLE I. Compilation of instances where a computational or machine learning prediction of a thermoelectric was later verified by experiment.

Year(s)	Composition	Method of prediction	Peak ZT in experiments	Notes
2006–2009	LiZnSb[90]	High-throughput DFT-based screening of 570 Sb-containing compounds from inorganic crystal structure database	ZT ranging from 0.02 to 0.08 (depending on direction) at ~525 K, p-type	Could not be doped n-type as required per prediction
2008–2015	NbFeSb[93–95]	DFT-based screening of 36 half-Heusler compositions	ZT of ~1.5 at 1200 K, p-type	A parallel high-throughput screening study, focusing more directly on this specific composition, reached zT ~ 1.0 at ~775 K
2014	SnS[96–99]	High-throughput screening >450 binary sulfides	ZT of ~0.6 at 873 K, p-type	History of this compound's identification is complex; doping optimization is crucial
2015	TmAgTe$_2$[100,101]	High-throughput DFT-based screening of ~48 000 compounds from the Materials Project database	ZT of 0.47 at ~700 K, p-type	Difficult to dope to desired carrier concentration, leading to inability to match theoretical max zT
2016	YCuTe$_2$[102]	Substitutions from above screening	ZT of 0.75 at 780 K, p-type	Experiment is close to prediction (zT ~ 0.82) when spin-orbit coupling effects are included
2016	Er$_{12}$Co$_5$Bi[103]	Machine learning recommendation engine	ZT ~0.07 at 600 K, n-type	First experimental tests of a purely machine learning prediction
2017	KAlSb$_4$[104]	DFT-based screening of 145 Zintl compounds	ZT ~0.7 at ~650 K, n-type	Experiment is very close to predicted maximum from theory
2018	Cd$_{1.6}$Cu$_{3.4}$In$_3$Te$_8$[105]	High-throughput DFT-based screening of 214 diamondlike systems in the Materials Innovation Platform database	ZT of 1.04 at 875 K, p-type	CdIn$_2$Te$_4$ was the initial hit in database screening; Cu intercalation to improve doping resulted in the final compound (never reported before)
2019	TaFeSb[106]	DFT-based screening of 27 half-Heusler compounds	ZT of 1.52 at 973 K, p-type	Compound never reported previously; computational screening focused on stability in half-Heusler phase rather than TE property optimization

coefficient (Fig. 2). However, one of the greatest practical limitations to current computational screening approaches is achieving the necessary carrier concentrations in experiments, typically through extrinsic doping. As Table I illustrates, the cases of LiZnSb and TmAgTe$_2$ are instances where the desired doping was never achieved, leading to much lower than expected ZT. In contrast, for YCuTe$_2$ and KAlSb, the desired carrier concentrations could be achieved and the experimental measurements of ZT were inline with calculated expectation. Dopability can, to some degree, be computed through a set of charged defect calculations,[118] but less computationally expensive and more chemically intuitive methods are needed. A major step forward would be to establish a large, high-quality dataset tabulating known dopabilities that could be used to test future theories.

Looking past theory-based screening, machine learning approaches present a new toolkit toward data-driven discovery. The investment into creating a Materials Genome[119] and other similar efforts have resulted in a series of online repositories that provide both general information (such as electronic and phonon band structures,)[120–125] as well as thermoelectric-specific databases.[126–129] These databases can serve as a training ground for machine learning

algorithms.[130] The choice of machine learning algorithm depends on the quality and quantity of data available in these datasets. One of the key challenges is to find suitable ways to vectorize data and create generally applicable basis sets that represent inorganic crystals.[131–133] Other inputs from density functional theory (DFT) calculations can be utilized as well[134] to predict thermoelectric properties. Then, supervised and unsupervised learning techniques can be used on these relatively sparse, yet informationally rich, datasets toward the prediction of new TE compounds. Clustering, dimensionality reduction, and other such techniques would help to understand the parameter space, while supervised learning techniques allow for classification and regression toward predictive performance, using meta estimators or neural network techniques, for instance. Initial approaches have shown predictive capacity[135] for the Seebeck coefficient or the power factor under a constant relaxation time.[134] In at least one instance (see Table I), a machine learning "recommendation engine" (similar to that of a movie or shopping recommendation algorithm) has suggested an atypical thermoelectric (Er$_{12}$Co$_5$Bi) that has been experimentally tested, albeit with low (<0.1) resulting figure of merit.[103]

One could even imagine a high-throughput experimental loop that can synthesize and characterize new materials at a rapid pace,
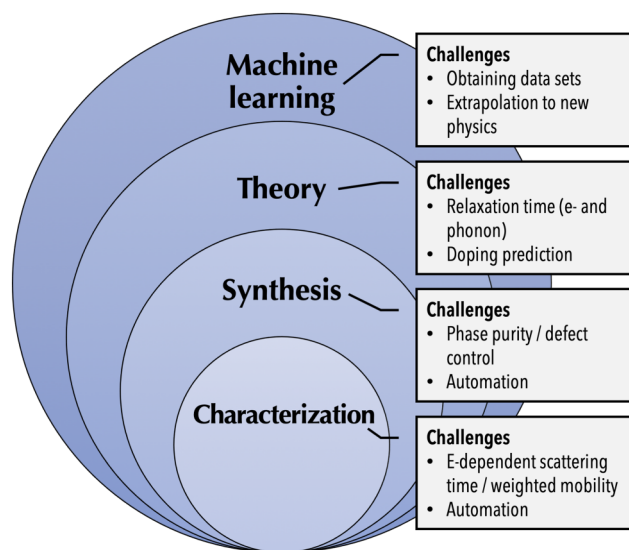
FIG. 5. A sequence of tools is now available to accelerate searches for materials candidates that meet desired thermoelectric performance criteria, starting from coarse machine learning models and ending in high fidelity characterization. However, challenges remain for all techniques as listed in the figure.

with machine learning embedded during the synthesis and characterization steps.[136,137] New experimental tools can be envisioned that can determine not only intrinsic transport parameters such as doping concentration, electrical conductivity, Seebeck coefficient, and Hall mobility using the method-of-four-coefficients, but also energy-dependent scattering times and the band-weighted mobility that can be directly compared with calculation. For thermal transport properties, time-domain thermoreflectance (TDTR), broadband frequency-domain thermoreflectance (FDTR), and transient thermal grating (TTG) not only determine the thermal conductivity but can also be used to glean thermal conductivity accumulation functions that give the mfp information for phonons. Such high-throughput experimental tools, in combination with synthesis routes such as co-sputtering, pulsed laser deposition (PLD), or metalorganic chemical vapor deposition (MOCVD)/MBE, and solution processable techniques can result in a large library of compounds that can act as good proxies to serve as a guide toward materials discovery. Such advances will help establish a more coherent approach that takes us from theoretical prediction (from inverse design) to theoretical and experimental screening toward accurate experiments, as illustrated in Fig. 5.

VII. CONCLUSIONS

Advances in applied physics typically emerge from new instrumentation, materials, or physical principles. The past few decades in thermoelectrics research have benefited enormously from new materials, precisely tailored to nanoscale dimensions in either superlattice or nanocrystal form, as well as from new optical and scanning-probe tools that have enabled investigation of microscale heat transport in

ways that were previously inconceivable. In this article, we argue for a new revolution in thermoelectrics driven by emerging concepts in condensed matter physics that have yet to be fully explored for thermal energy applications. These advances can be found in several prominent areas of applied physics relevant to thermoelectrics by re-examining, from first principles, the fundamental rules that have confined materials development for so long: the single-particle phonon gas picture with simple or constant relaxation times. Breaking these boundaries will enable new horizons in thermoelectrics to emerge. The wavelike nature of phonons, for example, could enable localization of thermal energy while allowing electrical carriers to remain itinerant heat pumps, thereby massively enhancing *ZT*. Several other prominent areas are highlighted that are promising contributors to the evolving landscape of thermoelectric materials design—correlated electron physics, polaronic transport in soft materials, and machine learning.

REFERENCES

[1]See https://flowcharts.llnl.gov/commodities/energy for LLNL Sankey energy flow diagrams for the USA.
[2]See https://arpa-e.energy.gov/sites/default/files/Joseph%20King%20Opening%20-Overview%20Waste%20Heat%20-%20For%20Posting_Revised.pdf for low temperature waste heat report, ARPA-E.
[3]A. K. Menon and S. K. Yee, J. Appl. Phys. **119**(5), 055501 (2016).
[4]A. K. Menon, O. Meek, A. J. Eng, and S. K. Yee, J. Appl. Polym. Sci. **134**(3), 44060 (2017).
[5]K. Gordiz, A. K. Menon, and S. K. Yee, J. Appl. Phys. **122**(12), 124507 (2017).
[6]K. Nan, S. D. Kang, K. Li, K. J. Yu, F. Zhu, J. Wang, A. C. Dunn, C. Zhou, Z. Xie, M. T. Agne, H. Wang, H. Luan, Y. Zhang, Y. Huang, G. J. Snyder, and J. A. Rogers, Sci. Adv. **4** (11), eaau5849 (2018).
[7]L. K. Allison and T. L. Andrew, Adv. Mater. Technol. **0**(0), 1800615 (2019).
[8]H. M. Elmoughni, A. K. Menon, R. M. W. Wolfe, and S. K. Yee, Adv. Mater. Technol. **0**(0), 1800708 (2019).
[9]C. Chang, M. Wu, D. He, Y. Pei, C.-F. Wu, X. Wu, H. Yu, F. Zhu, K. Wang, Y. Chen, L. Huang, J.-F. Li, J. He, and L.-D. Zhao, Science **360**(6390), 778 (2018).
[10]S. I. Kim, K. H. Lee, H. A. Mun, H. S. Kim, S. W. Hwang, J. W. Roh, D. J. Yang, W. H. Shin, X. S. Li, Y. H. Lee, G. J. Snyder, and S. W. Kim, Science **348**(6230), 109 (2015).
[11]H. Liu, X. Yuan, P. Lu, X. Shi, F. Xu, Y. He, Y. Tang, S. Bai, W. Zhang, L. Chen, Y. Lin, L. Shi, H. Lin, X. Gao, X. Zhang, H. Chi, and C. Uher, Adv. Mater. **25**(45), 6607–6612 (2013).
[12]J.-S. Rhyee, K. H. Lee, S. M. Lee, E. Cho, S. I. Kim, E. Lee, Y. S. Kwon, J. H. Shim, and G. Kotliar, Nature **459**, 965 (2009).

[13]V. K. Zaitsev, M. I. Fedorov, E. A. Gurieva, I. S. Eremin, P. P. Konstantinov, A. Y. Samunin, and M. V. Vedernikov, Phys. Rev. B **74**(4), 045207 (2006).

[14]S. Sakurada and N. Shutoh, Appl. Phys. Lett. **86**(8), 082105 (2005).

[15]K. F. Hsu, S. Loo, F. Guo, W. Chen, J. S. Dyck, C. Uher, T. Hogan, E. K. Polychroniadis, and M. G. Kanatzidis, Science **303**(5659), 818 (2004).

[16]B. C. Sales, D. Mandrus, and R. K. Williams, Science **272**(5266), 1325 (1996).

[17]O. Bubnova, Z. U. Khan, A. Malti, S. Braun, M. Fahlman, M. Berggren, and X. Crispin, Nat. Mater. **10**, 429 (2011).

[18]Y. Hiroshige, M. Ookawa, and N. Toshima, Synth. Met. **157**(10), 467–474 (2007).

[19]G. H. Kim, L. Shao, K. Zhang, and K. P. Pipe, Nat. Mater. **12**, 719 (2013).

[20]Y. Sun, L. Qiu, L. Tang, H. Geng, H. Wang, F. Zhang, D. Huang, W. Xu, P. Yue, Y.-s. Guan, F. Jiao, Y. Sun, D. Tang, C.-a. Di, Y. Yi, and D. Zhu, Adv. Mater. **28**(17), 3351–3358 (2016).

[21]M. Sumino, K. Harada, M. Ikeda, S. Tanaka, K. Miyazaki, and C. Adachi, Appl. Phys. Lett. **99**(9), 093308 (2011).

[22]Y. Sun, P. Sheng, C. Di, F. Jiao, W. Xu, D. Qiu, and D. Zhu, Adv. Mater. **24**(7), 932–937 (2012).

[23]K. C. See, J. P. Feser, C. E. Chen, A. Majumdar, J. J. Urban, and R. A. Segalman, Nano Lett. **10**(11), 4664–4667 (2010).

[24]H. Ju and J. Kim, ACS Nano **10**(6), 5730–5739 (2016).

[25]L. Wang, Z. Zhang, Y. Liu, B. Wang, L. Fang, J. Qiu, K. Zhang, and S. Wang, Nat. Commun. **9**(1), 3817 (2018).

[26]B. Zhang, J. Sun, H. E. Katz, F. Fang, and R. L. Opila, ACS Appl. Mater. Interfaces **2**(11), 3170–3178 (2010).

[27]J. H. We, S. J. Kim, and B. J. Cho, Energy **73**, 506–512 (2014).

[28]L. Wang, Z. Zhang, L. Geng, T. Yuan, Y. Liu, J. Guo, L. Fang, J. Qiu, and S. Wang, Energy Environ. Sci. **11**(5), 1307–1317 (2018).

[29]M. S. Dresselhaus, G. Dresselhaus, X. Sun, Z. Zhang, S. B. Cronin, and T. Koga, Phys. Solid State **41**(5), 679–682 (1999).

[30]A. J. Minnich, M. S. Dresselhaus, Z. F. Ren, and G. Chen, Energy Environ. Sci. **2**(5), 466–479 (2009).

[31]Z. Tian, S. Lee, and G. Chen, J. Heat Transfer **135**(6), 061605–061615 (2013).

[32]L.-D. Zhao, S.-H. Lo, Y. Zhang, H. Sun, G. Tan, C. Uher, C. Wolverton, V. P. Dravid, and M. G. Kanatzidis, Nature **508**, 373 (2014).

[33]A. A. Olvera, N. A. Moroz, P. Sahoo, P. Ren, T. P. Bailey, A. A. Page, C. Uher, and P. F. P. Poudeu, Energy Environ. Sci. **10**(7), 1668–1676 (2017).

[34]C. Kittel, *Introduction to Solid State Physics* (Wiley, 2004).

[35]L. D. Hicks and M. S. Dresselhaus, Phys. Rev. B **47**(19), 12727–12731 (1993).

[36]K. Hippalgaonkar, Y. Wang, Y. Ye, D. Y. Qiu, H. Zhu, Y. Wang, J. Moore, S. G. Louie, and X. Zhang, Phys. Rev. B **95**(11), 115407 (2017).

[37]J. He and T. M. Tritt, Science **357**(6358), eaak9997 (2017).

[38]B. Qiu, Z. Tian, A. Vallabhaneni, B. Liao, J. M. Mendoza, O. D. Restrepo, X. Ruan, and G. Chen, Europhys. Lett. **109**(5), 57006 (2015).

[39]X. Wang, V. Askarpour, J. Maassen, and M. Lundstrom, J. Appl. Phys. **123**(5), 055104 (2018).

[40]G. S. Kumar, G. Prasad, and R. O. Pohl, J. Mater. Sci. **28**(16), 4261–4272 (1993).

[41]R. W. McKinney, P. Gorai, V. Stevanović, and E. S. Toberer, J. Mater. Chem. A **5**(33), 17302–17311 (2017).

[42]N. Wakeham, A. F. Bangura, X. Xu, J.-F. Mercure, M. Greenblatt, and N. E. Hussey, Nat. Commun. **2**, 396 (2011).

[43]J. Crossno, J. K. Shi, K. Wang, X. Liu, A. Harzheim, A. Lucas, S. Sachdev, P. Kim, T. Taniguchi, K. Watanabe, T. A. Ohki, and K. C. Fong, Science **351**(6277), 1058 (2016).

[44]A. Weathers, Z. U. Khan, R. Brooke, D. Evans, M. T. Pettes, J. W. Andreasen, X. Crispin, and L. Shi, Adv. Mater. **27**(12), 2101–2106 (2015).

[45]N. Lu, L. Li, N. Gao, and M. Liu, J. Appl. Phys. **120**(19), 195108 (2016).

[46]S. Lee, K. Hippalgaonkar, F. Yang, J. Hong, C. Ko, J. Suh, K. Liu, K. Wang, J. J. Urban, X. Zhang, C. Dames, S. A. Hartnoll, O. Delaire, and J. Wu, Science **355**(6323), 371 (2017).

[47]S. A. Hartnoll, Nat. Phys. **11**, 54 (2014).

[48]P. D. Ronney, Combust. Flame **82**(1), 1–14 (1990).

[49]J. Ravichandran, A. K. Yadav, R. Cheaito, P. B. Rossen, A. Soukiassian, S. J. Suresha, J. C. Duda, B. M. Foley, C.-H. Lee, Y. Zhu, A. W. Lichtenberger, J. E. Moore, D. A. Muller, D. G. Schlom, P. E. Hopkins, A. Majumdar, R. Ramesh, and M. A. Zurbuchen, Nat. Mater. **13**, 168 (2013).

[50]M. N. Luckyanova, J. Garg, K. Esfarjani, A. Jandl, M. T. Bulsara, A. J. Schmidt, A. J. Minnich, S. Chen, M. S. Dresselhaus, Z. Ren, E. A. Fitzgerald, and G. Chen, Science **338**(6109), 936 (2012).

[51]M. N. Luckyanova, J. Mendoza, H. Lu, B. Song, S. Huang, J. Zhou, M. Li, Y. Dong, H. Zhou, J. Garlow, L. Wu, B. J. Kirby, A. J. Grutter, A. A. Puretzky, Y. Zhu, M. S. Dresselhaus, A. Gossard, and G. Chen, Sci. Adv. **4**(12), eaat9460 (2018).

[52]Z. Tian, K. Esfarjani, and G. Chen, Phys. Rev. B **89**(23), 235307 (2014).

[53]T. Albrecht, H. Arora, V. Ayanoor-Vitikkate, J.-M. Beaujour, D. Bedau, D. Berman, A. Bogdanov, Y. A. Chapuis, J. Cushen, E. Dobisz, G. Doerk, H. Gao, M. Grobis, B. Gurney, W. Hanson, O. Hellwig, T. Hirano, P. O. Jubert, D. Kercher, and E. Yang, "Bit patterned magnetic recording: Theory, media fabrication, and recording performance," IEEE Trans. Magn. **51**, 0800342 (2015).

[54]S. Dallorto, D. Staaks, A. Schwartzberg, X. Yang, K. Y. Lee, I. W. Rangelow, S. Cabrini, and D. L. Olynick, Nanotechnology **29**(40), 405302 (2018).

[55]David C. Bell, "Editorial: Special issue on helium ion microscopy," Scanning **34**(2), 81–82 (2012).

[56]C. R. Kagan and C. B. Murray, Nat. Nanotechnol. **10**, 1013 (2015).

[57]C. L. Poyser, T. Czerniuk, A. Akimov, B. T. Diroll, E. A. Gaulding, A. S. Salasyuk, A. J. Kent, D. R. Yakovlev, M. Bayer, and C. B. Murray, ACS Nano **10**(1), 1163–1169 (2016).

[58]T. Juntunen, O. Vänskä, and I. Tittonen, Phys. Rev. Lett. **122**(10), 105901 (2019).

[59]Z. Tian, ACS Nano **13**(4), 3750–3753 (2019).

[60]J. Billy, V. Josse, Z. Zuo, A. Bernard, B. Hambrecht, P. Lugan, D. Clément, L. Sanchez-Palencia, P. Bouyer, and A. Aspect, Nature **453**, 891 (2008).

[61]M. B. Zanjani and J. R. Lukes, J. Phys. Chem. C **119**(29), 16889–16896 (2015).

[62]O. Bubnova and X. Crispin, Energy Environ. Sci. **5**(11), 9345–9362 (2012).

[63]S. Wang, M. Ha, M. Manno, C. Daniel Frisbie, and C. Leighton, Nat. Commun. **3**, 1210 (2012).

[64]H. T. Yi, Y. N. Gartstein, and V. Podzorov, Sci. Rep. **6**, 23650 (2016).

[65]M. Cutler and N. F. Mott, Phys. Rev. **181**(3), 1336–1340 (1969).

[66]H. Fritzsche, Science **176**(4039), 1117 (1972).

[67]R. Noriega, J. Rivnay, K. Vandewal, F. P. V. Koch, N. Stingelin, P. Smith, M. F. Toney, and A. Salleo, Nat. Mater. **12**, 1038 (2013).

[68]C. Li, H. Ma, and Z. Tian, Appl. Therm. Eng. **111**, 1441–1447 (2017).

[69]S. A. Gregory, A. K. Menon, S. Ye, D. S. Seferos, J. R. Reynolds, and S. K. Yee, Adv. Energy Mater. **8**(34), 1802419 (2018).

[70]A. M. Glaudell, J. E. Cochran, S. N. Patel, and M. L. Chabinyc, Adv. Energy Mater. **5**(4), 1401072 (2015).

[71]B. Russ, A. Glaudell, J. J. Urban, M. L. Chabinyc, and R. A. Segalman, Nat. Rev. Mater. **1**, 16050 (2016).

[72]S. D. Kang and G. J. Snyder, Nat. Mater. **16**, 252 (2016).

[73]O. Bubnova, M. Berggren, and X. Crispin, J. Am. Chem. Soc. **134**(40), 16456–16459 (2012).

[74]D. Venkateshvaran, M. Nikolka, A. Sadhanala, V. Lemaur, M. Zelazny, M. Kepa, M. Hurhangee, A. J. Kronemeijer, V. Pecunia, I. Nasrallah, I. Romanov, K. Broch, I. McCulloch, D. Emin, Y. Olivier, J. Cornil, D. Beljonne, and H. Sirringhaus, Nature **515**, 384 (2014).

[75]B. Russ, M. J. Robb, F. G. Brunetti, P. L. Miller, E. E. Perry, S. N. Patel, V. Ho, W. B. Chang, J. J. Urban, M. L. Chabinyc, C. J. Hawker, and R. A. Segalman, Adv. Mater. **26**(21), 3473–3477 (2014).

[76]A. K. Menon, R. M. W. Wolfe, S. R. Marder, J. R. Reynolds, and S. K. Yee, Adv. Funct. Mater. **28**(29), 1801620 (2018).

[77]R. M. W. Wolfe, A. K. Menon, T. R. Fletcher, S. R. Marder, J. R. Reynolds, and S. K. Yee, Adv. Funct. Mater. **28**(37), 1803275 (2018).

[78]W. Shi, G. Wu, K. Hippalgaonkar, J.-S. Wang, J. Xu, and S.-W. Yang, J. Am. Chem. Soc. **140**(41), 13200–13204 (2018).

[79] R. M. W. Wolfe, A. K. Menon, S. R. Marder, J. R. Reynolds, and S. K. Yee, Adv. Electron. Mater. **0**(0), 1900066 (2019).

[80] A. K. Menon, R. M. W. Wolfe, S. Kommandur, and S. K. Yee, Adv. Electron. Mater. **0**(0), 1800884 (2019).

[81] D. J. Bergman and O. Levy, J. Appl. Phys. **70**(11), 6821–6833 (1991).

[82] D. J. Bergman and L. G. Fel, J. Appl. Phys. **85**(12), 8205–8216 (1999).

[83] J. Sun, M. L. Yeh, B. J. Jung, B. Zhang, J. Feser, A. Majumdar, and H. E. Katz, Macromolecules **43**(6), 2897–2903 (2010).

[84] G. Zuo, X. Liu, M. Fahlman, and M. Kemerink, ACS Appl. Mater. Interfaces **10**(11), 9638–9644 (2018).

[85] E. S. Cho, N. E. Coates, J. D. Forster, A. M. Ruminski, B. Russ, A. Sahu, N. C. Su, F. Yang, and J. J. Urban, Adv. Mater. **27**(38), 5744–5752 (2015).

[86] J.-H. Bahk, Z. Bian, and A. Shakouri, Phys. Rev. B **87**(7), 075204 (2013).

[87] P. Kumar, E. W. Zaia, E. Yildirim, D. V. M. Repaka, S.-W. Yang, J. J. Urban, and K. Hippalgaonkar, Nat. Commun. **9**(1), 5347 (2018).

[88] N. P. Blake and H. Metiu, in *Chemistry, Physics, and Materials Science of Thermoelectric Materials: Beyond Bismuth Telluride*, edited by M. G. Kanatzidis, S. D. Mahanti, and T. P. Hogan (Springer US, Boston, MA, 2003), pp. 259–302.

[89] A. Jain, Y. Shin, and K. A. Persson, Nat. Rev. Mater. **1**, 15004 (2016).

[90] G. K. H. Madsen, J. Am. Chem. Soc. **128**(37), 12140–12146 (2006).

[91] E. S. Toberer, A. F. May, C. J. Scanlon, and G. J. Snyder, J. Appl. Phys. **105**(6), 063701 (2009).

[92] J. Park, Y. Xia, and V. Ozoliņš, Phys. Rev. Appl. **11**(1), 014058 (2019).

[93] C. Fu, S. Bai, Y. Liu, Y. Tang, L. Chen, X. Zhao, and T. Zhu, Nat. Commun. **6**, 8144 (2015).

[94] J. Yang, H. Li, T. Wu, W. Zhang, L. Chen, and J. Yang, Adv. Funct. Mater. **18**(19), 2880–2888 (2008).

[95] G. Joshi, R. He, M. Engber, G. Samsonidze, T. Pantha, E. Dahal, K. Dahal, J. Yang, Y. Lan, B. Kozinsky, and Z. Ren, Energy Environ. Sci. **7**(12), 4070–4076 (2014).

[96] Q. Tan, L.-D. Zhao, J.-F. Li, C.-F. Wu, T.-R. Wei, Z.-B. Xing, and M. G. Kanatzidis, J. Mater. Chem. A **2**(41), 17302–17306 (2014).

[97] C. Bera, S. Jacob, I. Opahle, N. S. H. Gunda, R. Chmielowski, G. Dennler, and G. K. H. Madsen, Phys. Chem. Chemi. Phys. **16**(37), 19894–19899 (2014).

[98] D. Parker and D. J. Singh, J. Appl. Phys. **108**(8), 083712 (2010).

[99] M. M. Nassary, J. Alloys Compd. **398**(1), 21–25 (2005).

[100] J.-H. Pöhls, Z. Luo, U. Aydemir, J.-P. Sun, S. Hao, J. He, I. G. Hill, G. Hautier, A. Jain, X. Zeng, C. Wolverton, G. J. Snyder, H. Zhu, and M. A. White, J. Mater. Chem. A **6**(40), 19502–19519 (2018).

[101] H. Zhu, G. Hautier, U. Aydemir, Z. M. Gibbs, G. Li, S. Bajaj, J.-H. Pöhls, D. Broberg, W. Chen, A. Jain, M. A. White, M. Asta, G. J. Snyder, K. Persson, and G. Ceder, J. Mater. Chem. C **3**(40), 10554–10565 (2015).

[102] U. Aydemir, J.-H. Pöhls, H. Zhu, G. Hautier, S. Bajaj, Z. M. Gibbs, W. Chen, G. Li, S. Ohno, D. Broberg, S. D. Kang, M. Asta, G. Ceder, M. A. White, K. Persson, A. Jain, and G. J. Snyder, J. Mater. Chem. A **4**(7), 2461–2472 (2016).

[103] M. W. Gaultois, A. O. Oliynyk, A. Mar, T. D. Sparks, G. J. Mulholland, and B. Meredig, APL Mater. **4**(5), 053213 (2016).

[104] B. R. Ortiz, P. Gorai, L. Krishna, R. Mow, A. Lopez, R. McKinney, V. Stevanović, and E. S. Toberer, J. Mater. Chem. A **5**(8), 4036–4046 (2017).

[105] L. Xi, S. Pan, X. Li, Y. Xu, J. Ni, X. Sun, J. Yang, J. Luo, J. Xi, W. Zhu, X. Li, D. Jiang, R. Dronskowski, X. Shi, G. J. Snyder, and W. Zhang, J. Am. Chem. Soc. **140**(34), 10785–10793 (2018).

[106] H. Zhu, J. Mao, Y. Li, J. Sun, Y. Wang, Q. Zhu, G. Li, Q. Song, J. Zhou, Y. Fu, R. He, T. Tong, Z. Liu, W. Ren, L. You, Z. Wang, J. Luo, A. Sotnikov, J. Bao, K. Nielsch, G. Chen, D. J. Singh, and Z. Ren, Nat. Commun. **10**(1), 270 (2019).

[107] G. K. H. Madsen, J. Carrete, and M. J. Verstraete, Comput. Phys. Commun. **231**, 140–145 (2018).

[108] A. Togo and I. Tanaka, Scr. Mater. **108**, 1–5 (2015).

[109] W. Li, J. Carrete, N. A. Katcho, and N. Mingo, Comput. Phys. Commun. **185**(6), 1747–1758 (2014).

[110] S. Poncé, E. R. Margine, C. Verdi, and F. Giustino, Comput. Phys. Commun. **209**, 116–133 (2016).

[111] X. Wang, E. Witkoske, J. Maassen, and M. Lundstrom, e-print arXiv:1806.08888 (2018).

[112] P. Gorai, V. Stevanović, and E. S. Toberer, Nat. Rev. Mater. **2**, 17053 (2017).

[113] W. Chen, J.-H. Pöhls, G. Hautier, D. Broberg, S. Bajaj, U. Aydemir, Z. M. Gibbs, H. Zhu, M. Asta, G. J. Snyder, B. Meredig, M. A. White, K. Persson, and A. Jain, J. Mater. Chem. C **4**(20), 4414–4426 (2016).

[114] R. P. Chasmar and R. Stratton, J. Electron. Control **7**(1), 52–72 (1959).

[115] G. D. Mahan, in *Solid State Physics*, edited by H. Ehrenreich and F. Spaepen (Academic Press, 1998), **51**, pp. 81–157.

[116] J. Yan, P. Gorai, B. Ortiz, S. Miller, S. A. Barnett, T. Mason, V. Stevanović, and E. S. Toberer, Energy Environ. Sci. **8**(3), 983–994 (2015).

[117] Z. M. Gibbs, F. Ricci, G. Li, H. Zhu, K. Persson, G. Ceder, G. Hautier, A. Jain, and G. J. Snyder, npj Comput. Mater. **3**(1), 8 (2017).

[118] C. Freysoldt, B. Grabowski, T. Hickel, J. Neugebauer, G. Kresse, A. Janotti, and C. G. Van de Walle, Rev. Mod. Phys. **86**(1), 253–305 (2014).

[119] A. White, MRS Bull. **37**(8), 715–716 (2012).

[120] A. Jain, S. P. Ong, G. Hautier, W. Chen, W. D. Richards, S. Dacek, S. Cholia, D. Gunter, D. Skinner, G. Ceder, and K. A. Persson, APL Mater. **1**(1), 011002 (2013).

[121] S. Curtarolo, W. Setyawan, S. Wang, J. Xue, K. Yang, R. H. Taylor, L. J. Nelson, G. L. W. Hart, S. Sanvito, M. Buongiorno-Nardelli, N. Mingo, and O. Levy, Comput. Mater. Sci. **58**, 227–235 (2012).

[122] S. Kirklin, J. E. Saal, B. Meredig, A. Thompson, J. W. Doak, M. Aykol, S. Rühl, and C. Wolverton, npj Comput. Mater. **1**, 15010 (2015).

[123] G. Pizzi, A. Cepellotti, R. Sabatini, N. Marzari, and B. Kozinsky, Comput. Mater. Sci. **111**, 218–230 (2016).

[124] B. Blaiszik, K. Chard, J. Pruyne, R. Ananthakrishnan, S. Tuecke, and I. Foster, JOM **68**(8), 2045–2052 (2016).

[125] X. Yang, Z. Wang, X. Zhao, J. Song, M. Zhang, and H. Liu, Comput. Mater. Sci. **146**, 319–333 (2018).

[126] F. Ricci, W. Chen, U. Aydemir, G. J. Snyder, G.-M. Rignanese, A. Jain, and G. Hautier, Sci. Data **4**, 170085 (2017).

[127] P. Gorai, D. Gao, B. Ortiz, S. Miller, S. A. Barnett, T. Mason, Q. Lv, V. Stevanović, and E. S. Toberer, Comput. Mater. Sci. **112**, 368–376 (2016).

[128] J. Carrete, N. Mingo, S. Wang, and S. Curtarolo, Adv. Funct. Mater. **24**(47), 7427–7432 (2014).

[129] M. W. Gaultois, T. D. Sparks, C. K. H. Borg, R. Seshadri, W. D. Bonificio, and D. R. Clarke, Chem. Mater. **25**(15), 2911–2920 (2013).

[130] A. Jain, G. Hautier, S. P. Ong, and K. Persson, J. Mater. Res. **31**(8), 977–994 (2016).

[131] T. Xie and J. C. Grossman, Phys. Rev. Lett. **120**(14), 145301 (2018).

[132] L. Ward, A. Agrawal, A. Choudhary, and C. Wolverton, npj Comput. Mater. **2**, 16028 (2016).

[133] C. Chen, W. Ye, Y. Zuo, C. Zheng, and S. P. Ong, e-print arXiv:1812.05055 (2018).

[134] L. Laugier, D. Bash, J. Recatala, H. K. Ng, S. Ramasamy, C.-S. Foo, V. R. Chandrasekhar, and K. Hippalgaonkar, e-print arXiv:1811.06219 (2018).

[135] A. o. Furmanchuk, J. E. Saal, J. W. Doak, G. B. Olson, A. Choudhary, and A. Agrawal, J. Comput. Chem. **39**(4), 191–202 (2018).

[136] E. M. Chan, C. Xu, A. W. Mao, G. Han, J. S. Owen, B. E. Cohen, and D. J. Milliron, Nano Lett. **10**(5), 1874–1885 (2010).

[137] S. Steiner, J. Wolf, S. Glatzel, A. Andreou, J. M. Granda, G. Keenan, T. Hinkley, G. Aragon-Camarasa, P. J. Kitson, D. Angelone, and L. Cronin, Science **363**(6423), eaav2211 (2019).